trans positions, Figure 5. Such crystallographic conformational constraints are typical of many monosubstituted regular metallocene complexes, as in $[Mn(Me_3SiC_5H_4)_2]$,[35] which is both isostructural and isomorphous with 4.

Important geometrical parameters are given in Table II. The average Mg–C(ring) distance is 2.336 Å, corresponding to a Mg–centroid distance of 2.00 Å, which compares with the Mg–centroid and Mg–C(ring) distances of 2.011 (8), 2.008 (4) and 2.341 (6), 2.339 (4) Å, respectively, observed in the gas-phase structures of $[Mg(C_5Me_5)_2]$[7] and $[Mg(C_5H_5)_2]$,[23] but are significantly longer than the Mg–C(average) bond distances found in the crystal structure of $[Mg(C_5H_5)_2]$,[22] 1.96 and 2.304 Å, respectively. The heavily substituted complex, $[Mg\{\eta^5\text{-}1,2,4\text{-}(SiMe_3)_3C_5H_2\}_2]$,[25] has a longer average Mg–centroid distance of 2.03 Å. This complex also exhibits nonparallel cyclopentadienyl rings and considerable deviations of the trimethylsilyl substituents from the plane of the cyclopentadienyl rings, presumably a consequence of steric interactions between the ligands. The cyclopentadienyl compound, $[Mg\{\eta^5\text{-}1,2,4\text{-}(SiMe_3)_3C_5H_2\}Br(TMEDA)]$,[25] displays yet a larger average Mg–centroid distance of 2.167 Å, as does the analogous unsubstituted complex, $[Mg(\eta^5\text{-}C_5H_5)Br(TMEDA)]$, ca. 2.21 Å (TMEDA = *N,N,N′,N′*-tetramethylethylenediamine).[36]

Acknowledgment. We gratefully acknowledge support of this work by the Australian Research Council.

Supplementary Material Available: Tables SUP1–SUP11, listing thermal parameters, ligand hydrogen parameters, metal core geometries, and ligand non-hydrogen geometries for **1b**, **2b**, and 4 (10 pages); tables of structure factor amplitudes (26 pages). Ordering information is given on any current masthead page.

---

[35] Hebendanz, N.; Köhler, F. H.; Müller, G.; Riede, J. *J. Am. Chem. Soc.* **1986**, *108*, 3281.

[36] Johnson, C.; Toney, J.; Stucky, G. D. *J. Organomet. Chem.* **1972**, *40*, C11.

---

^{59}Co NMR Study of Cluster Reactions: Solvent and Ligand Effects in Mixed-Metal, Tetrahedral MCo_3 (M = Fe, Ru) Carbonyl Clusters. Crystal Structure of $FeCo_3(\mu_3\text{-}H)(\mu\text{-}CO)_3(CO)_8(PPh_2H)$

Pierre Braunstein* and Jacky Rosé

Laboratoire de Chimie de Coordination, URA 416 CNRS, Université Louis Pasteur,
4 rue Blaise Pascal, 67070 Strasbourg Cédex, France

Pierre Granger and Jésus Raya

Unité Mixte 50 CNRS-Bruker-ULP, Université Louis Pasteur, BP 296/R8, 67008 Strasbourg Cédex, France

Salah-Eddine Bouaoud and Daniel Grandjean

Laboratoire de Cristallochimie, URA 254, Université de Rennes 1, Avenue du Général Leclerc,
35042 Rennes Cédex, France

Received February 25, 1991

^{59}Co NMR spectroscopy is used to study the site selectivity of reactions between tetrahedral mixed-metal clusters $HMCo_3(CO)_{12}$ (M = Fe (**1a**), M = Ru (**1b**)) and various 2e donor ligands. In the monosubstituted clusters $HMCo_3(CO)_{11}L$ [M = Fe, L = PPh_2H (**2a**), PCy_2H (**4a**), PPh_3 (**5a**), NMe_3 (**6a**), SEt_2 (**7a**); M = Ru, L = PPh_2H (**2b**), PCy_2H (**4b**), PPh_3 (**5b**)] the ligand L is bound to a basal Co atom, generally giving rise to two ^{59}Co NMR resonances in a 2:1 ratio. The variation in chemical shift is examined throughout the series. The reaction of **2a** with a slight excess of Me_3NO in CH_2Cl_2 was monitored by ^{59}Co NMR spectroscopy and gave $HFeCo_3(CO)_{10}(NMe_3)(PPh_2H)$ (**8a**), in which each of the three chemically different Co atoms gives rise to a different resonance. This labile cluster transforms first to **2a** and then to the anion $[FeCo_3(CO)_{11}(PPh_2H)]^-$, owing to decoordination of the amine. Deprotonation of cluster **2a** also occurs in solvents like THF or acetone, which deprotonate the more acidic clusters **1a** or **1b** even more readily. Comparisons are made between disubstituted $FeCo_3$ clusters containing (P, P), (P, N), or (P, S) monodentate donor ligands, which illustrate the sensitivity of ^{59}Co NMR spectroscopy and its diagnostic value for the study of metallosite selectivity in cluster reactions. The structure of **2a** has been determined by X-ray diffraction: space group $P\bar{1}$ with a = 14.615 (5) Å, b = 17.087 (2) Å, c = 11.136 (3) Å, α = 99.20 (1)°, β = 105.94 (2)°, γ = 87.49 (2)°, and Z = 4. The structure was refined to R = 0.029 and R_w = 0.041 on the basis of 5764 reflections having $F_o^2 > 3\sigma(F_o^2)$. There are two independent, almost identical molecules in the asymmetric unit. The cluster has a tetrahedral structure and the phosphine is axially bonded to a basal cobalt atom. The triply bridging hydride ligand was found to be closer to the cobalt atom bearing the PPh_2H ligand.

Introduction

Reactivity studies on mixed-metal cluster compounds require appropriate monitoring and unambiguous identification of the reaction products. This usually involves the use of infrared (particularly for carbonyl clusters) and ^{1}H, ^{13}C, or ^{31}P NMR spectroscopy. Here, we wish to illustrate the potential of ^{59}Co NMR spectroscopy,[1] which has been little used in cluster chemistry.[2]

---

[1] (a) Kidd, R. G.; Goodfellow, R. J. In *NMR and the Periodic Table*; Harris, R. K., Mann, B. E., Eds.; Academic Press: New York, 1978. (b) Laszlo, P. In *NMR of Newly Accessible Nuclei*; Laszlo, P., Ed.; Academic Press: New York, 1983; Vol. 2.

0276-7333/91/2310-3686$02.50/0

Table I. Selected Infrared and ^{59}Co NMR Data

	IR	NMR
cluster	ν(CO), cm^{-1} (CH_2Cl_2)	^{59}Co, δ ($\Delta\nu_{1/2}$, Hz)[a]
$HFeCo_3(CO)_{12}$ (**1a**)	2060 vs, 2052 vs, 2030 m, 1990 m, 1887 s[b]	−2720 (420) (CoCO)[c]
$[Et_4N][FeCo_3(CO)_{12}]$	2069 w, 2010 vs, 1968 m, 1928 m, 1811 m	−2600 (2250) (CoCO)[c]
$HRuCo_3(CO)_{12}$ (**1b**)	2067 s, 2024 m, 1879 m	−2760 (1700) (CoCO)
$[Et_4N][RuCo_3(CO)_{12}]$	2060 w, 2019 s, 2002 s, 1966 m, 1805 m	−2645 (565) (CoCO)[d]
$HFeCo_3(CO)_{11}(PPh_2H)$ (**2a**)	2082 m, 2039 vs, 2014 vs, 1969 m, 1895 sh, 1864 m, 1853 m	−2718 (1500) (CoCO) −2615 (1500) (CoP)
$HRuCo_3(CO)_{11}(PPh_2H)$ (**2b**)	2088 m, 2051 vs, 2015 vs, 1980 sh, 1861 m, 1850 sh	−2736 (2550) (CoCO in A)[e] −2862 (4900) (CoP in A) −2693 (3300) (CoCO in B) −2794 (4800) (CoP in B)
$HFeCo_3(CO)_{10}(PPh_2H)_2$ (**3a**)	2079 vs, 2043 vs, 2023 vs, 1971 m, 1936 w, 1886 w, 1857 s, 1838 s[b]	−2695 (2300) (CoCO) −2549 (2000) (CoP)
$HFeCo_3(CO)_{11}(PCy_2H)$ (**4a**)	2081 m, 2041 vs, 2014 vs, 1973 m, 1940 vw, 1896 w, 1872 m, 1855 m[b]	−2697 (1400) (CoCO) −2632 (2100) (CoP)
$HRuCo_3(CO)_{11}(PCy_2H)$ (**4b**)	2088 m, 2048 vs, 2037 vs, 2017 vs, 1990 w, 1980 w, 1893 w, 1872 m, 1856 m	−2708 (3600) (CoCO + CoP)
$HFeCo_3(CO)_{11}(PPh_3)$ (**5a**)	2085 m, 2042 vs, 2015 s, 1970 m, 1866 m, 1850 m	−2690 (1500) (CoCO)[c] −2467 (1600) (CoP)
$HRuCo_3(CO)_{11}(PPh_3)$ (**5b**)	2088 m, 2042 s, 2015 s, 1863 m, 1847 m	−2710 (4400) (CoCO) −2564 (2800) (CoP)
$HFeCo_3(CO)_{11}(NMe_3)$ (**6a**)	2080 m, 2033 vs, 2003 vs, 1967 sh, 1866 s, 1845 s	−2730 (800) (CoCO) −910 (3200) (CoN)
$HFeCo_3(CO)_{11}(SEt_2)$ (**7a**)	2085 w, 2040 vs, 2015 s, 1967 m, 1896 sh, 1864 m, 1851 m	−2725 (1100) (CoCO) −1831 (3000) (CoS)
$HFeCo_3(CO)_{10}(NMe_3)(PPh_2H)$ (**8a**)	2081m, 2056 s, 2038 vs, 2020 vs, 1996 vs, 1867 sh, 1839 m, 1820 m	−2717 (1500) (CoCO) −2531 (1500) (CoP) −783 (6000) (CoN)
$HFeCo_3(CO)_{10}(PPh_2H)(SEt_2)$ (**9a**)	2062 s, 2039 m, 2027 vs, 2005 vs, 1976 w, 1963 w, 1872 w, 1846 m, 1829 m[b]	−2714 (1700) (CoCO) −2572 (1700) (CoP) −1764 (5000) (CoS)
$[Et_3NH][FeCo_3(CO)_{11}(PPh_2H)]$ (**10a**)	2041 m, 1988 vs, 1964 s, 1913 m, 1794 m	−2562 (7000) (CoCO) f
$[Et_4N][FeCo_3(CO)_{11}(PPh_3)]$ (**11a**)	2033 m, 1985 vs, 1957 s, 1913 m, 1795 m	−2484 (3700) (CoCO) −2160 (8500) (CoP)

[a] Measured at 298 K in $CDCl_3$; sample concentrations 1–2 × 10^{-2} mol/L; ref $K_3[Co(CN)_6]$ in D_2O; the line widths are not meaningful since they contain relaxation effects and coupling constants. [b] Recorded in hexane. [c] Recorded in CD_2Cl_2. [d] Recorded in acetone-d_6. [e] Two isomers A and B are present, in comparable amounts, in solution (see text). [f] For the ^{59}CoP resonance, see text.

The site selectivity of ligand substitution in mixed-metal clusters remains an area of considerable interest. In a number of tetrahedral carbonyl clusters, the selectivity for apical versus basal substitution, which in the latter case may occur in an axial or equatorial position, has been investigated by spectroscopic methods and X-ray diffraction.[3] Although reactions with phosphine ligands have been extensively studied, relatively little is known about the reactivity of secondary phosphines, PR_2H. This could lead to simple CO substitution or formation of a μ-PR_2 bridge via P–H oxidative addition, as also observed with, for example, trinuclear clusters.[4] Reactions at hydrido clusters are of particular interest as PR_2H may act as a base[5] or could react via its P–H bond with the M–H functionality to eliminate H_2 and form phosphido clusters. There is only one crystal structure reported (Cambridge Crystallographic Data Base) of a tetranuclear hydrido cluster containing a PPh_2H ligand, that of the tetrahedral cluster $CpNiOs_3(\mu\text{-}H)_3(CO)_8(PPh_2H)$.[6] We set out to study such ligand substitution reactions on a family of $FeCo_3$ and $RuCo_3$ carbonyl clusters of continuing structural and chemical interest.[3b,5,7] The fact that these clusters afforded high-quality ^{59}Co NMR spectra within a few minutes of recording on a high-field spectrometer, together with the sensitivity of ^{59}Co NMR chemical shifts to small chemical changes, prompted us to report that this technique allows an easy differentiation between Co atoms whose chemical inequivalence results from the replacement of a neighboring metal atom or of a CO by another 2e donor ligand.

Results and Discussion

The reaction of $HMCo_3(CO)_{12}$ (**1a**, M = Fe; **1b**, M = Ru) with 1 equiv of PPh_2H at room temperature rapidly afforded the monosubstituted derivatives $HMCo_3(CO)_{11}(PPh_2H)$ (**2a**, M = Fe; **2b**, M = Ru), which were characterized by analytical and spectroscopic data (Table I) and by an X-ray diffraction study of **2a** (see below). Changing the stoichiometry and the reaction conditions allows the isolation of $HMCo_3(CO)_{10}(PPh_2H)_2$ (**3a**, M = Fe; **3b**, M = Ru) and, in the case of M = Fe, of a small amount of green $Co_3(\mu\text{-}PPh_2)_3(CO)_6$.[8] Similarly, the clusters $HMCo_3(CO)_{11}(PCy_2H)$ (**4a**, M = Fe; **4b**, M = Ru) were prepared and isolated. The IR data (ν(CO) region) for these complexes are compared in Table I with those for the PPh_3 analogues **5a** and **5b**, respectively. The appropriate choice of solvent is crucial as basic solvents such as acetone or THF may deprotonate such hydrido clusters, as previously described for **1a**.[9a] Deprotonation is also observed here

---

(2) (a) Saito, T.; Sawada, S. *Bull. Chem. Soc. Jpn.* **1985**, *58*, 459. (b) Hidai, M.; Matsuzaka, H.; Koyasu, Y.; Uchida, Y. *J. Chem. Soc., Chem. Commun.* **1986**, 1451. (c) Matsuzaka, H.; Kodama, T.; Uchida, Y.; Hidai, M. *Organometallics* **1988**, *7*, 1608. (d) Hidai, M.; Matsuzaka, H. *Polyhedron* **1988**, *7*, 2369. (e) Ching, S.; Sabat, M.; Shriver, D. F. *Organometallics* **1989**, *8*, 1047.

(3) (a) Bojczuk, M.; Heaton, B. T.; Johnson, S.; Ghilardi, C. A.; Orlandini, A. *J. Organomet. Chem.* **1988**, *341*, 473. (b) Pursiainen, J.; Pakkanen, T. A. *Acta Chem. Scand.* **1989**, *43*, 463. (c) Pursiainen, J.; Ahlgren, M.; Pakkanen, T. A.; Valkonen, J. *J. Chem. Soc., Dalton Trans.* **1990**, 1147.

(4) (a) Iwasaki, F.; Mays, M. J.; Raithby, P. R.; Taylor, P. L.; Wheatley, P. J. *J. Organomet. Chem.* **1981**, *213*, 185. (b) Colbran, S. B.; Johnson, B. F. G.; Lewis, J.; Sorrell, R. M. *J. Organomet. Chem.* **1985**, *296*, C1. (c) Patel, V. D.; Cherkas, A. A.; Nucciarone, D.; Taylor, N. J.; Carty, A. J. *Organometallics* **1985**, *4*, 1792.

(5) Cooke, C. G.; Mays, M. J. *J. Chem. Soc., Dalton Trans.* **1975**, 455.

(6) Predieri, G.; Tiripicchio, A.; Vignali, C.; Sappa, E.; Braunstein, P. *J. Chem. Soc., Dalton Trans.* **1986**, 1135.

(7) Pakkanen, T. A.; Pursiainen, J.; Venäläinen, T.; Pakkanen, T. T. *J. Organomet. Chem.* **1989**, *372*, 129.

(8) Dale Harley, A.; Guskey, G. J.; Geoffroy, G. L. *Organometallics* **1983**, *2*, 53.

for **1b** (see below, ^{59}Co NMR studies) and **2a** (complete conversion into [{THF}H]$^+$[$FeCo_3(CO)_{11}(PPh_2H)$]$^-$ within ca. 3 h, which was characterized by comparison with an authentic sample of [Et_4N][$FeCo_3(CO)_{11}(PPh_3)$],[10] see below). The stability of the phosphine-substituted anionic clusters in solution is limited by their progressive transformation to [$FeCo_3(CO)_{12}$]$^-$.

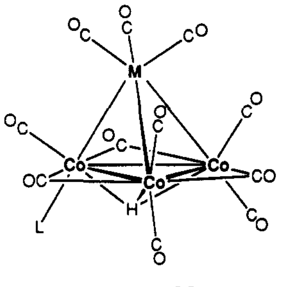

1a M = Fe, L = CO
1b M = Ru, L = CO
2a M = Fe, L = PPh_2H
2b M = Ru, L = PPh_2H
4a M = Fe, L = PCy_2H
4b M = Ru, L = PCy_2H
5a M = Fe, L = PPh_3
5b M = Ru, L = PPh_3
6a M = Fe, L = NMe_3
7a M = Fe, L = SEt_2

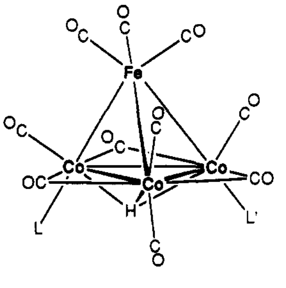

3a L = L' = PPh_2H
8a L = NMe_3; L' = PPh_2H
9a L = SEt_2; L' = PPh_2H

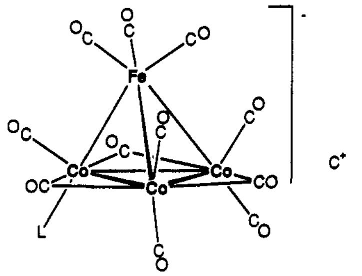

10a L = PPh_2H, C = Et_3NH
11a L = PPh_3, C = Et_4N

Amine-substituted clusters are very useful synthetic intermediates[11] but are rarely amenable to solid-state characterization. The reaction of excess trimethylamine *N*-oxide, Me_3NO, with a CH_2Cl_2 solution of **1a** allowed quantitative formation and isolation of $HFeCo_3(CO)_{11}(NMe_3)$ (**6a**), which is stable in the solid state.[12] This cluster reacts within a few minutes with 1 equiv of PPh_2H or PPh_3 in CH_2Cl_2 to give **2a** or **5a**, respectively. It reacts more slowly with 1–2 equiv of SEt_2 ($t_{1/2} \approx 15$ h) to give $HFeCo_3(CO)_{11}(SEt_2)$ (**7a**) in high yields. Interestingly, **2a** reacted instantaneously with Me_3NO in CH_2Cl_2 to afford $HFeCo_3(CO)_{10}(NMe_3)(PPh_2H)$ (**8a**). This cluster is very labile, as shown by IR monitoring, both in toluene or CH_2Cl_2 and in the solid state, but surprisingly transforms first into **2a** without any sign of oxidative addition of the P–H bond. It appears therefore that the amine ligand dissociates from **8a** and that some CO must be liberated by partial decomposition of the cluster to readily occupy the vacant coordination site, thus regenerating **2a**. Owing to the presence of the liberated amine, deprotonation of **2a** subsequently occurs and yields the anion [$FeCo_3(CO)_{11}(PPh_2H)$]$^-$, also observed in the solvent-induced deprotonation reactions of **2a** (vide supra). Only [Et_3NH][$FeCo_3(CO)_{11}(PPh_2H)$] (**10a**) was isolated from the reaction of **2a** with NEt_3 in CH_2Cl_2.

The reaction leading to **8a** constitutes an unambiguous example where oxidation of a cluster-bound CO by Me_3NO leads to the corresponding amino derivative with complete metallosite selectivity (Co versus Fe). The lability of the newly formed Co–amine bond may be exploited for the selective preparation of other disubstituted clusters. Thus, reaction of **2a** with Me_3NO in CH_2Cl_2, in the presence of a slight excess of SEt_2, afforded $HFeCo_3(CO)_{10}(PPh_2H)(SEt_2)$ (**9a**), which is more stable than **8a** and may be isolated pure in the solid state. Although all the species formed have well-defined IR spectra in the ν(CO) region, it is often difficult to analyze complex mixtures owing to overlaping absorptions. This calls for an additional analytical method, and ^{59}Co NMR has proved very useful.

Spectroscopic ^{59}Co NMR Studies. In a nonpolar solvent such as CD_2Cl_2, **1a** and **1b**[2] give rise to a single resonance for their three equivalent Co atoms at −2720 and −2760 ppm, respectively (Table I). The acidity of **1a** toward Lewis base solvents such as ethanol, acetone, or THF[9] is now also evidenced for **1b**. This emphasizes the considerable importance of the choice of the NMR solvents when studying such clusters.[12] Thus, deprotonation of **1a** and **1b** in acetone was monitored by the shift toward lower wavenumbers of the IR ν(CO) absorptions and by the emergence of new ^{59}Co NMR resonances at ca. −2600 and −2640 ppm, respectively. These values correspond to the chemical shifts of authentic samples of the anionic clusters [$MCo_3(CO)_{12}$]$^-$, M = Fe and Ru, respectively (Table I). Therefore, the resonance at −2648 ppm assigned previously by Hidai et al.[2b,c] to **1b** in acetone corresponds in fact to [$RuCo_3(CO)_{12}$]$^-$. In the structurally related cluster $Co_4(CO)_{12}$, which is isoelectronic with **1**, two Co resonances are observed in CD_2Cl_2 in a 1:3 intensity ratio. These fall at −690 and −2080 ppm (cf. −715 and −2065 ppm in $CDCl_3$[13]) and are assigned to the apical and basal Co atoms, respectively. Note that the changes in the capping fragment of the tetrahedral MCo_3 core maintained the equivalence of the three Co atoms.

In contrast, substitution of a CO ligand in **1a** or **1b** by a phosphine ligand should give rise to two Co resonances, since the phoshine ligand is bound to cobalt in $HMCo_3(CO)_{11}(PPh_3)$ (**5a**, M = Fe; **5b**, M = Ru).[2b,5] This is indeed observed (Table I), with an accidental overlap of these resonances in **4b** (see below). The resonances at −2690 ppm in **5a** and −2710 ppm in **5b** are similar to those observed in their corresponding precursors and are therefore assigned to the unsubstituted Co atoms. In contrast, those at −2467 and −2564 ppm, respectively, are assigned to the phosphine-substituted Co atom; a result that is also in agreement with their relative intensities (Table I). Varying the phosphine results in significant modifications of the chemical shift for the substituted Co site, as observed when comparing, e.g., **2a** and **5a** (difference of ca. 148 ppm), whereas the other cobalt nuclei remain almost unperturbed. Replacing Fe with Ru mostly affects the resonance of the phosphine-substituted Co nucleus, as seen when comparing **5a** with **5b** (difference of ca. 97 ppm). The occurrence of a shift of this magnitude between **4a** and **4b** could account for the observation of only one ^{59}Co resonance in **4b**. This effect might be due to the position

---

[9] (a) Aime, S.; Osella, D.; Milone, L.; Manotti Lanfredi, A.-M.; Tiripicchio, A. *Inorg. Chim. Acta* **1983**, *71*, 141. (b) Chini, P.; Colli, L.; Peraldo, M. *Gazz. Chim. Ital.* **1960**, *90*, 1005.

[10] Cooke, C. G.; Mays, M. J. *J. Organomet. Chem.* **1974**, *74*, 449.

[11] (a) Albers, M. O.; Coville, N. J. *Coord. Chem. Rev.* **1984**, *53*, 227. (b) Luh, T.-Y. *Ibid.* **1984**, *60*, 255. (c) Shen, J.-K., Gao, Y.-C.; Shi, Q.-Z.; Basolo, F. *Organometallics* **1989**, *8*, 2144.

[12] (a) Braunstein, P.; Mourey, L.; Rosé, J.; Granger, P.; Richert, T., unpublished results. (b) Braunstein, P.; Rosé, J.; Granger, P.; Richert, T. *Magn. Reson. Chem.*, in press.

[13] Aime, S.; Gobetto, R.; Osella, D.; Milone, L.; Hawkes, G. E.; Randall, E. W. *J. Magn. Reson.* **1985**, *65*, 308.

occupied by the phosphine ligand, transoid to the apical metal center. The observation of two sets of resonances for **2b** is consistent with the presence of two isomers A and B in solution. The spectroscopic similarity indicates closely related structures for these isomers. Our best suggestion at the moment is that the phosphine ligand may be axially or equatorially coordinated to the cobalt center. In support of this hypothesis we note that in $HRuRh_3(CO)_{11}(PR_3)$ the phosphine ligand may occupy an axial or an equatorial site.[3b,c]

Two Co resonances were also observed for $[Et_4N][FeCo_3(CO)_{11}(PPh_3)]$ (**11a**), that assigned to the phosphine-substituted Co nuclei at −2160 ppm being much broader ($\Delta\nu_{1/2} \sim 8500$ Hz) than that at −2484 ppm ($\Delta\nu_{1/2} \sim 3700$ Hz), which is assigned to the two equivalent Co nuclei. It is interesting to note that the Co resonances of the phosphine-substituted clusters are shifted to higher frequencies when going from the hydrido to the anionic derivatives. A similar trend is observed for the corresponding unsubstituted clusters, e.g., **1a** versus $[Et_4N][FeCo_3(CO)_{12}]$. When going from **11a** to $[Et_3NH][FeCo_3(CO)_{11}(PPh_2H)]$ (**10a**), the resonances of the equivalent cobalt nuclei (CoCO) at −2562 ppm becomes much broader ($\Delta\nu_{1/2} \sim 7000$ Hz) (see Table I). The CoP resonance was not observed, probably owing to further broadening of the already broad resonance observed for **11a**.

The lability of amine-substituted clusters makes in situ ^{59}Co NMR monitoring of their reactions of considerable interest. The reaction of excess Me_3NO with a $CDCl_3$ solution of **2a** rapidly led to two resonances at −2531 and −783 ppm, which could be assigned to **8a** by comparison with an authentic sample, the resonance of the unsubstituted Co nucleus remaining at ca. −2717 ppm. The instability of **8a** (see above), which leads to rapid regeneration of **2a**, may be conveniently monitored by the observation of the resonances of the latter at ca. −2718 and −2615 ppm, these being the only resonances present after ca. 3 h (Figure 1). After ca. 48 h, these resonances disappear and are replaced with new ones at ca. −3025 ($[Co(CO)_4]^-$), −2608 ($[FeCo_3(CO)_{12}]^-$), and −2553 ppm (unsubstituted Co nuclei of $[FeCo_3(CO)_{11}(PPh_2H)]^-$, similar to the value for **10a**). The resonance at −783 ppm in **8a**, assigned to the amine-substituted cobalt atom, should be compared with that at −910 ppm found in **6a**. This shows the sensitivity of this nucleus to replacement of CO by PPh_2H at a neighboring cobalt site. Conversely, the resonance at −2531 ppm in **8a** is shifted by ca. 84 ppm by comparison with that of the phosphine-substituted cobalt in **2a** (−2615 ppm), illustrating the effect of replacing the amine by CO at the neighboring Co center. In these systems, the chemical shifts of the unsubstituted Co atoms are little affected by substitution by either a phosphine or an amine at one Co neighbor (see **2a** and **6a**) or at each Co neighbor in the disubstituted clusters (see **3a** and **8a**).

Similar results were observed in the reaction of **5a** with Me_3NO in $CDCl_3$, which was performed in an NMR tube for direct monitoring. New ^{59}Co NMR resonances were observed at −737 ($CoNMe_3$), −2308 ($CoPPh_3$) and −2664 (CoCO) ppm and were assigned to $HFeCo_3(CO)_{10}(NMe_3)(PPh_3)$. This cluster is very labile and could not be isolated pure in the solid state. Its ruthenium analogue was also spectroscopically characterized and displays ^{59}Co NMR resonances at −920 ($CoNMe_3$), −2370 ($CoPPh_3$) and −2650 (CoCO) ppm, whereas $HRuCo_3(CO)_{10}(NMe_3)(PPh_2H)$ could only be detected [by $\delta(CoNMe_3) = -990$] owing to its even greater lability. Although we have no X-ray diffraction data for **3a**, **8a**, and **9a**, we draw their structures with the ligands L and L′ in axial positions, by analogy with the situation found in $HRuCo_3(CO)_{10}(PPh_3)_2$.[14]

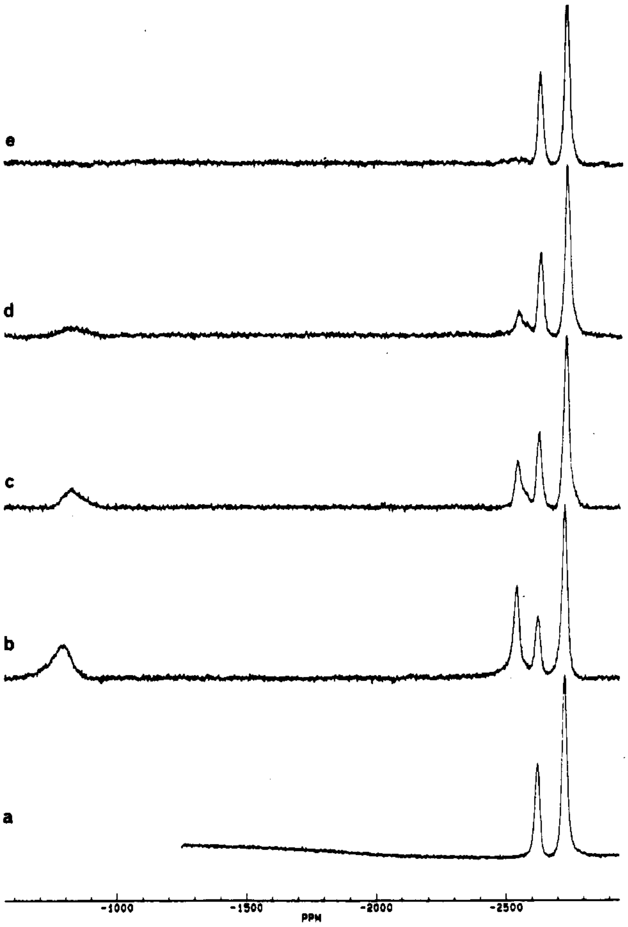

Figure 1. ^{59}Co NMR monitoring of the reaction of **2a** with Me_3NO in $CDCl_3$ showing the rapid formation of **8a** and its progressive disappearance with reformation of **2a**. (a) Pure **2a**, (b) after reaction time $t = 5$ min, (c) $t = 30$ min, (d) $t = 1$ h, (e) $t = 3$ h. Spectra b–d are those of a mixture of **2a** and **8a**.

In **9a**, the values of the ^{59}Co NMR resonances (Table I) are typical for an unsubstituted Co nucleus (−2714 ppm), a phosphine-substituted Co (−2572 ppm), and a thioether-substituted Co (−1764 ppm). They illustrate the diagnostic value and sensitivity of ^{59}Co NMR to ligand replacement in this series of clusters. The sensitivity to phosphine substitution is even more pronounced in trimetallic Fe_2Co clusters as shown when going from $[PPN][Fe_2Co(CO)_9(\mu_3\text{-}CCO)]$ with $\delta = -2670$ to $[PPN][Fe_2Co(CO)_8(PEt_3)(\mu_3\text{-}CCO)]$ with $\delta = -1560$.[2e]

Crystal Structure of $FeCo_3(\mu_3\text{-}H)(\mu\text{-}CO)_3(CO)_8(PPh_2H)$ (2a). Two independent, almost identical molecules of **2a** are present in the asymmetric unit. Figure 2 shows a perspective view of this cluster and relevant bond lengths and angles are given in Tables II and III, respectively. The Fe–Co and Co–Co distances in this tetrahedral cluster are in the range found for these bonds in the related molecules $[FeCo_3(CO)_{11}(PPh_3)]^-$,[15b] $FeCo_3(\mu_3\text{-}AuPPh_3)(CO)_{12}$,[15] $FeCo_3(\mu_3\text{-}AuPPh_3)(CO)_{11}(PMe_2Ph)$,[15b] and $FeCo_3(\mu_3\text{-}H)(CO)_9[P(OMe)_3]_3$.[16] A carbonyl ligand bridges

---

[14] Pursiainen, J.; Pakkanen, T. A.; Jääskeläinen, J. *J. Organomet. Chem.* 1985, *290*, 85.

[15] (a) Lauher, J. W.; Wald, K. *J. Am. Chem. Soc.* 1981, *103*, 7648. (b) Low, A. A.; Lauher, J. W. *Inorg. Chem.* 1987, *26*, 3863.

[16] (a) Hure, B. T.; Knobler, C. B.; Kaesz, H. D. *J. Am. Chem. Soc.* 1978, *100*, 3059. (b) Teller, R. G.; Wilson, R. D.; McMullan, R. K.; Koetzle, T. F.; Bau, R. *Ibid.* 1978, *100*, 3071.

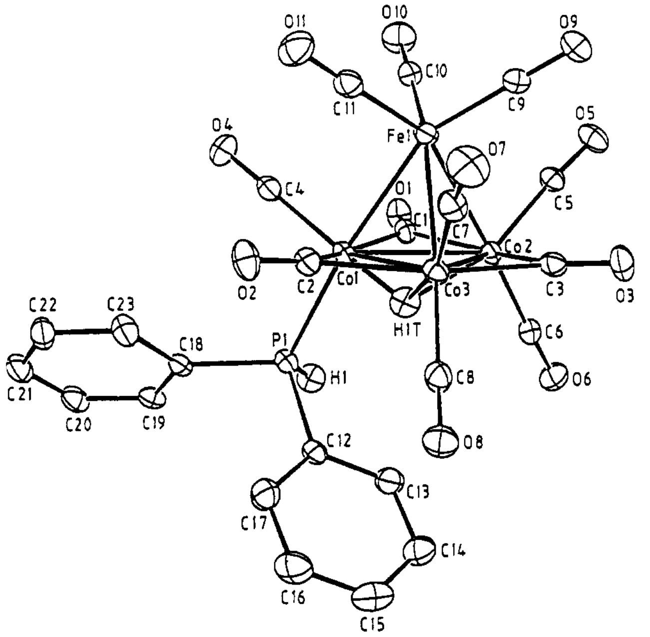

Figure 2. View of the molecular structure of one molecule of **2a** with the atom labeling scheme.

Table II. Selected Bond Distances (Å) for 2a[a]

molecule A			molecule B		
Co1	Fe1	2.543 (1)	Co4	Fe2	2.552 (1)
Co2	Fe1	2.555 (1)	Co5	Fe2	2.561 (1)
Co3	Fe1	2.535 (1)	Co6	Fe2	2.536 (1)
Co1	Co2	2.491 (1)	Co4	Co5	2.487 (1)
Co1	Co3	2.494 (1)	Co4	Co6	2.496 (1)
Co2	Co3	2.499 (1)	Co5	Co6	2.494 (1)
Co1	P1	2.223 (1)	Co4	P2	2.226 (1)
Co1	C1	1.936 (4)	Co4	C24	1.941 (5)
Co1	C2	1.914 (4)	Co4	C25	1.920 (5)
Co1	C4	1.765 (5)	Co4	C27	1.747 (5)
Co1	H1T	1.37 (4)	Co4	H2T	1.57 (4)
Co2	C1	1.972 (5)	Co5	C24	1.954 (5)
Co2	C3	1.976 (5)	Co5	C26	1.973 (5)
Co2	C5	1.774 (5)	Co5	C29	1.768 (5)
Co2	C6	1.797 (5)	Co5	C28	1.817 (5)
Co2	H1T	1.78 (4)	Co5	H2T	1.76 (4)
Co3	C2	2.008 (4)	Co6	C25	2.006 (4)
Co3	C3	1.967 (5)	Co6	C26	1.966 (5)
Co3	C7	1.773 (6)	Co6	C31	1.762 (5)
Co3	C8	1.806 (5)	Co6	C30	1.804 (5)
Co3	H1T	1.78 (4)	Co6	H2T	1.73 (4)
Fe1	C9	1.799 (5)	Fe2	C33	1.808 (5)
Fe1	C10	1.797 (5)	Fe2	C32	1.790 (5)
Fe1	C11	1.789 (5)	Fe2	C34	1.792 (5)
P1	H1	1.35 (4)	P2	H2	1.34 (4)
P1	C12	1.808 (4)	P2	C41	1.817 (5)
P1	C18	1.808 (4)	P2	C35	1.800 (4)
O1	C1	1.150 (5)	O24	C24	1.157 (5)
O2	C2	1.151 (5)	O25	C25	1.141 (5)
O3	C3	1.144 (5)	O26	C26	1.136 (5)
O4	C4	1.129 (5)	O27	C27	1.145 (6)
O5	C5	1.134 (5)	O29	C29	1.133 (5)
O6	C6	1.131 (5)	O28	C28	1.113 (6)
O7	C7	1.124 (6)	O31	C31	1.137 (5)
O8	C8	1.120 (5)	O30	C30	1.133 (6)
O9	C9	1.130 (5)	O33	C33	1.128 (5)
O10	C10	1.131 (5)	O32	C32	1.138 (5)
O11	C11	1.140 (5)	O34	C34	1.129 (5)

[a] Numbers in parentheses are estimated standard deviations in the least significant digits.

each Co–Co bond: C(3)O(3) in a symmetrical manner, whereas C(1)O(1) and C(2)O(2) are slightly closer to the phosphine-substituted Co atom. The axial disposition of the PPh_2H ligand is as anticipated and is comparable to

Table III. Selected Bond Angles (deg) for 2a[a]

molecule A				molecule B			
Co2	Co1	Fe1	61.00 (2)	Co5	Co4	Fe2	61.09 (2)
Co3	Co1	Fe1	60.43 (2)	Co6	Co4	Fe2	60.32 (2)
Co1	Co2	Fe1	60.50 (2)	Co4	Co5	Fe2	60.70 (2)
Co3	Co2	Fe1	60.21 (2)	Co6	Co5	Fe2	60.19 (2)
Co1	Co3	Fe1	60.73 (2)	Co4	Co6	Fe2	60.95 (2)
Co2	Co3	Fe1	60.99 (2)	Co5	Co6	Fe2	61.21 (2)
Co1	Fe1	Co2	58.51 (2)	Co4	Fe2	Co5	58.21 (2)
Co1	Fe1	Co3	58.83 (2)	Co4	Fe2	Co6	58.74 (2)
Co2	Fe1	Co3	58.80 (2)	Co5	Fe2	Co6	58.59 (2)
Co1	Co3	Co2	59.86 (2)	Co4	Co6	Co5	59.80 (2)
Co1	Co2	Co3	59.98 (2)	Co4	Co5	Co6	60.12 (2)
Co2	Co1	Co3	60.17 (2)	Co5	Co4	Co6	60.08 (2)
Fe1	Co1	P1	173.29 (4)	Fe2	Co4	P2	174.51 (4)
Fe1	Co1	C1	81.0 (1)	Fe2	Co4	C24	81.7 (1)
Fe1	Co1	C2	82.3 (1)	Fe2	Co4	C25	83.2 (1)
Fe1	Co1	C4	89.6 (2)	Fe2	Co4	C27	87.0 (2)
Fe1	Co1	H1T	89 (2)	Fe2	Co4	H2T	89 (2)
Fe1	Co2	C1	80.0 (1)	Fe2	Co5	C24	81.2 (1)
Fe1	Co2	C3	82.8 (1)	Fe2	Co5	C26	82.2 (1)
Fe1	Co2	C5	81.2 (1)	Fe2	Co5	C29	79.9 (1)
Fe1	Co2	C6	177.8 (2)	Fe2	Co5	C28	179.7 (2)
Fe1	Co2	H1T	81 (1)	Fe2	Co5	H2T	84 (1)
Fe1	Co3	C2	80.8 (1)	Fe2	Co6	C25	82.0 (1)
Fe1	Co3	C3	83.5 (1)	Fe2	Co6	C26	83.0 (1)
Fe1	Co3	C7	81.4 (2)	Fe2	Co6	C31	78.6 (2)
Fe1	Co3	C8	177.2 (1)	Fe2	Co6	C30	175.5 (2)
Fe1	Co3	H1T	81 (1)	Fe2	Co6	H2T	86 (1)
Co1	Fe1	C9	156.3 (2)	Co4	Fe2	C33	156.1 (2)
Co1	Fe1	C10	99.5 (2)	Co4	Fe2	C32	98.9 (2)
Co1	Fe1	C11	99.4 (2)	Co4	Fe2	C34	100.5 (2)
Co2	Fe1	C9	101.0 (2)	Co5	Fe2	C33	100.8 (2)
Co2	Fe1	C10	102.3 (2)	Co5	Fe2	C32	102.2 (2)
Co2	Fe1	C11	153.7 (2)	Co5	Fe2	C34	154.3 (2)
Co3	Fe1	C9	101.4 (2)	Co6	Fe2	C33	101.8 (2)
Co3	Fe1	C10	156.0 (2)	Co6	Fe2	C32	155.4 (2)
Co3	Fe1	C11	98.7 (2)	Co6	Fe2	C34	99.1 (2)
Co1	Co2	C1	49.8 (2)	Co4	Co5	C24	50.1 (1)
Co1	Co2	C3	110.4 (1)	Co4	Co5	C26	110.6 (1)
Co1	Co2	C5	130.1 (2)	Co4	Co5	C29	128.4 (1)
Co1	Co2	C6	117.7 (1)	Co4	Co5	C28	119.6 (2)
Co1	Co2	H1T	32 (1)	Co4	Co5	H2T	39 (1)
Co3	Co2	C1	109.5 (1)	Co6	Co5	C24	110.0 (1)
Co3	Co2	C3	50.5 (1)	Co6	Co5	C26	50.6 (1)
Co3	Co2	C5	127.5 (1)	Co6	Co5	C29	127.4 (1)
Co3	Co2	C6	120.5 (1)	Co6	Co5	C28	119.7 (2)
Co3	Co2	H1T	45 (1)	Co6	Co5	H2T	44 (1)
Co2	Co1	P1	113.51 (4)	Co5	Co4	P2	114.06 (2)
Co2	Co1	C1	51.0 (1)	Co5	Co4	C24	50.5 (1)
Co2	Co1	C2	112.3 (1)	Co5	Co4	C25	112.1 (1)
Co2	Co1	C4	132.6 (2)	Co5	Co4	C27	132.3 (2)
Co2	Co1	H1T	44 (2)	Co5	Co4	H2T	45 (2)
Co2	Co3	C2	108.6 (2)	Co5	Co6	C25	108.8 (1)
Co2	Co3	C3	50.8 (1)	Co5	Co6	C26	50.8 (1)
Co2	Co3	C7	128.8 (2)	Co5	Co6	C31	127.0 (2)
Co2	Co3	C8	121.2 (2)	Co5	Co6	C30	123.2 (2)
Co2	Co3	H1T	45 (1)	Co5	Co6	H2T	45 (1)
Co3	Co1	P1	113.95 (4)	Co6	Co4	P2	115.52 (4)
Co3	Co1	C1	110.9 (1)	Co6	Co4	C24	110.4 (1)
Co3	Co1	C2	52.2 (1)	Co6	Co4	C25	52.1 (1)
Co3	Co1	C4	137.7 (2)	Co6	Co4	C27	134.5 (2)
Co3	Co1	H1T	44 (2)	Co6	Co4	H2T	43 (2)
Co1	C4	O4	176.5 (4)	Co4	C27	O27	176.9 (5)
Co1	C2	O2	143.6 (4)	Co4	C25	O25	144.8 (4)
Co3	C2	O2	137.4 (4)	Co6	C25	O25	136.4 (4)
Co1	C1	O1	142.4 (4)	Co4	C24	O24	141.6 (4)
Co2	C1	O1	138.4 (4)	Co5	C24	O24	138.6 (4)
Co2	C5	O5	175.0 (4)	Co5	C29	O29	174.8 (4)
Co2	C6	O6	177.2 (4)	Co5	C28	O28	178.6 (5)
Co2	C3	O3	139.1 (4)	Co5	C26	O26	139.8 (4)
Co3	C3	O3	142.0 (4)	Co6	C26	O26	141.3 (4)
Co3	C7	O7	173.7 (5)	Co6	C31	O31	174.2 (5)
Co3	C8	O8	174.8 (5)	Co6	C30	O30	174.3 (5)
Co1	P1	C12	114.6 (1)	Co4	P2	C41	115.8 (2)
Co1	P1	C18	119.0 (2)	Co4	P2	C35	118.4 (2)
Co1	P1	H1	114 (2)	Co4	P2	H2	113 (2)

[a] Numbers in parentheses are estimated standard deviations in the least significant digits.

the situation in $RuCo_3(\mu_3\text{-}H)(CO)_{11}(PPh_3)$,[2c] although equatorial phosphines have been encountered in tetrahedral clusters.[3c] The Fe(1)Co(1)C(4) angle of 89.6 (2)° [for the second molecule 87.0 (2)°] is significantly larger than the other Fe–Co–C_{eq} angles. The Co–P distance of 2.223 (1) [2.226 (1)] Å is similar to that in $FeCo_3(\mu_3\text{-}AuPPh_3)(CO)_{11}(PMe_2Ph)$ [2.247 (9) Å][15b] but slightly shorter than in $RuCo_3(\mu_3\text{-}H)(CO)_{11}(PPh_3)$ [2.261 (5) Å].[2c] The P–H distance of 1.34 (4) [1.35 (4)] Å is significantly longer than in the other structurally characterized tetrahedral hydrido cluster containing a PPh_2H ligand: $CpNiOs_3(\mu\text{-}H)_3(CO)_8(PPh_2H)$ (1.10 Å).[6] The triply bridging hydride ligand could be located and is situated 0.756 (0.871) Å below the plane of the cobalt atoms, in excellent agreement with the analogous distance of ca. 0.75 Å observed in $FeCo_3(\mu_3\text{-}H)(CO)_9[P(OMe)_3]_3$.[16a] It is significantly closer to the cobalt atom bearing the phosphine substituent, which is consistent with the proton being closer to the more electron-rich metal center.

Conclusion

In view of the large number of homo- and heteronuclear cobalt-containing clusters of structural or catalytic interest,[17] ^{59}Co NMR spectroscopy should prove a very useful method to improve our knowledge about metallosite selectivity in cluster reactions. Direct monitoring of the successive reaction steps is of considerable interest in the fields of preparative chemistry and homogeneous catalysis. ^{59}Co NMR constitutes a most valuable tool for investigating complex reaction mixtures. It appears especially useful in combination with other spectroscopic techniques or methods where confusion may arise, e.g., overlap of IR ν(CO) bands of different species or decomposition on TLC plates. The surprisingly high quality of our ^{59}Co NMR spectra might be related to a "cluster effect" previously observed with other first-row transition elements.[18] Further studies are in progress.[12]

Experimental Section

General Procedures. Standard Schlenk line techniques were used, and manipulations were carried out under a purified nitrogen atmosphere. Solvents were distilled before use. $HFeCo_3(CO)_{12}$,[9b] $[Et_4N][FeCo_3(CO)_{11}(PPh_3)]$,[10] $[Et_4N][RuCo_3(CO)_{12}]$,[19] and $HRuCo_3(CO)_{11}(PPh_3)$[2c] were prepared by use of published procedures. All organophosphines were commercial samples and were used as received. Solution infrared spectra were recorded on a Perkin-Elmer 398 in 0.1-mm matched BaF_2 cells. NMR spectra were measured on a Bruker MSL-300 instrument (^{59}Co, 71.21 MHz). The chemical shifts reported (ppm) are positive high frequency from the external reference $K_3[Co(CN)_6]$ saturated in D_2O. Standard parameters are as follows: pulse width 3 μs, sweep width 263 kHz, number of scans between 5000 and 100 000. Spectroscopic data for the complexes are given in Table I. When product stability allowed, elemental analyses are given.

Preparation of $HRuCo_3(CO)_{12}$ (1b). $[Et_4N][RuCo_3(CO)_{12}]\cdot{}^1/_3$ THF (0.599 g, 0.778 mmol) was dissolved in acetone (20 mL) under stirring. HBF_4 (34% in water, 30 mL) was added slowly (ca. 10 drops/mn) at room temperature. Compound **1b** precipitated as a red microcrystalline solid. It was collected by filtration, washed with degassed water, and dried in vacuo. The isolated yield of **1b** was 0.380 g (79%). Anal. Calcd for $C_{12}HCo_3O_{12}Ru$: C, 23.44; H, 0.16. Found: C, 23.2; H, 0.2.

Preparation of $HFeCo_3(CO)_{11}(PPh_2H)$ (2a). To a solution of **1a** (0.517 g, 0.893 mmol) in a hexane/CH_2Cl_2 mixture (30 mL/15 mL), was added PPh_2H (0.157 mL, 0.913 mmol), and the reaction mixture was stirred for 1 h at room temperature. The violet solution was filtered, CH_2Cl_2 was evaporated, and the remaining solution, stored overnight at -20 °C, afforded **2a** as black crystals, which were filtered and dried in vacuo (0.350 g, 53%). Anal. Calcd for $C_{23}H_{12}Co_3FeO_{11}P$: C, 37.95; H, 1.66. Found: C, 38.2; H, 1.8.

Table IV. Crystal Data and Data Collection for 2a

formula	$C_{23}H_{12}FeCo_3O_{11}P$
fw	727.97
cryst system	triclinic
space group	$P\bar{1}$
cryst dimens, mm	0.2 × 0.15 × 0.10
cryst color	black
a, Å	14.615 (5)
b, Å	17.087 (2)
c, Å	11.136 (3)
α, deg	99.20 (1)
β, deg	105.94 (2)
γ, deg	87.49 (2)
V, Å^3	2639
Z	4
ρ_{calcd}, g/cm^3	1.832
$F(000)$	1440
temp. °C	25
diffractometer	Enraf-Nonius CAD-4
radiatn (graphite monochromator)	Mo Kα (λ 0.710 73 Å)
linear abs coeff, cm^{-1}	25.05
scan type	$\omega/2\theta$
scan width, deg	$1 + 0.35 \tan\theta$
θ limits, deg	1–24
systematic absences	none
octants collected	$\pm h,\pm k,l$
no. of data collected	8752
no. of unique data used	5764 [$F_o^2 > 3\sigma(F_o^2)$]
no. of variables	719
R $\sum(\lVert F_o\rvert - \lvert F_c\rVert)/\sum\lvert F_o\rvert$	0.029
R_w $[\sum w(\lvert F_o\rvert - \lvert F_c\rvert)^2/\sum w\lvert F_o\rvert^2]^{1/2}$	0.041
GOF = $[\sum w(\lvert F_o\rvert - \lvert F_c\rvert)^2/(N(\text{observns}) - N(\text{params}))]^{1/2}$	1.001
largest shift/esd, final cycle	0.23
largest peak in final diff map, e/Å^3	0.491
fudge factor	0.07

Preparation of $HRuCo_3(CO)_{11}(PPh_2H)$ (2b). To a solution of **1b** (0.320 g, 0.520 mmol) in hexane (20 mL), was added PPh_2H (0.090 mL, 0.523 mmol), and the reaction mixture was stirred for 0.5 h at room temperature. The resulting solution was filtered and chromatographed over silica gel, using hexane as eluant, which afforded four bands. The first fast-moving red band of residual **1b** was followed by a second red band of **2b** (0.085 g, 21%). Anal. Calcd for $C_{23}H_{12}Co_3O_{11}PRu$: C, 35.73; H, 1.56. Found: C, 35.8; H, 1.7. Further elution with hexane gave first a yellow band (unknown product) and then a dark red band, which afforded black microcrystals of $HRuCo_3(CO)_{10}(PPh_2H)_2$ (0.035 g, 7%).

Preparation of $HFeCo_3(CO)_{10}(PPh_2H)_2$ (3a). To a solution of **1a** (0.230 g, 0.403 mmol) in hexane (30 mL), was added a 2-fold excess of PPh_2H (0.140 mL, 0.809 mmol), and the reaction mixture was stirred for 2 h at room temperature. Chromatographic separation over silica gel, using a hexane–toluene mixture (9:1) as eluant, afforded three bands. A fast-moving purple band of residual **1a** and a violet band of **2a** (0.030 g) were followed by a yellow-green band that afforded $Co_3(\mu\text{-}PPh_2)_3(CO)_9$ in low yield.[8] When we used a 5:3 hexane–toluene mixture as eluant, a black-violet band followed, which yielded black crystals of **3a** (0.180 g, 50%). Anal. Calcd for $C_{34}H_{23}Co_3FeO_{10}P_2$: C, 46.09; H, 2.62. Found: C, 46.5; H, 2.6. The yield of the disubstituted cluster could be increased by longer reaction times.

Preparation of $HFeCo_3(CO)_{11}(PCy_2H)$ (4a). This cluster was prepared by the same procedure as for **2a**, but the resulting solution was filtered, evaporated to dryness, and chromatographed over silica gel to give black crystals of pure **4a**$\cdot{}^1/_3C_6H_{12}$ in 40% yield. Anal. Calcd for $C_{25}H_{28}Co_3FeO_{11}P$: C, 39.09; H, 3.67. Found: C, 38.8; H, 3.5.

Preparation of $HRuCo_3(CO)_{11}(PCy_2H)$ (4b). This cluster was prepared by the same procedure as for **2b**. Chromatographic separation gave black-red crystals of **4b**$\cdot{}^1/_2C_6H_{12}$ in good yield (68%), together with some unreacted **1b**. Anal. Calcd for

---

(17) Braunstein, P.; Rosé, J. Heterometallic Clusters in Catalysis. In *Stereochemistry of Organometallic and Inorganic Compounds*; Bernal, I., Ed.; Elsevier: Amsterdam, 1989; Vol. 3, pp 3–138.

(18) Rehder, D. *Magn. Reson. Rev.* **1984**, *9*, 125.

(19) Braunstein, P.; Rosé, J. *Inorg. Synth.* **1989**, *26*, 356.

Table V. Positional Parameters and Their Estimated Standard Deviations

atom	*x*	*y*	*z*	*B*,[a] Å^2	atom	*x*	*y*	*z*	*B*,[a] Å^2
Co1	0.20621 (4)	0.26381 (3)	0.61196 (5)	2.75 (1)	C10	0.3115 (3)	0.3149 (3)	0.9206 (4)	3.8 (1)
Co2	0.27558 (4)	0.14435 (3)	0.70581 (5)	2.90 (1)	C11	0.1247 (3)	0.3328 (3)	0.8605 (4)	4.1 (1)
Co3	0.09994 (4)	0.16731 (3)	0.65397 (5)	3.13 (1)	C12	0.1290 (3)	0.1757 (2)	0.3060 (4)	3.15 (9)
Co4	0.62600 (4)	0.23987 (3)	0.26218 (5)	3.00 (1)	C13	0.1651 (3)	0.0999 (3)	0.3056 (4)	4.6 (1)
Co5	0.55422 (4)	0.35912 (3)	0.36069 (5)	3.02 (1)	C14	0.1116 (4)	0.0354 (3)	0.2345 (5)	5.6 (1)
Co6	0.72952 (4)	0.33728 (3)	0.43007 (5)	3.15 (1)	C15	0.0209 (4)	0.0470 (3)	0.1618 (5)	5.8 (1)
Fe1	0.20782 (4)	0.25573 (3)	0.83854 (5)	3.09 (1)	C16	−0.0145 (4)	0.1221 (3)	0.1621 (5)	5.9 (1)
Fe2	0.62054 (4)	0.24849 (3)	0.49101 (5)	3.22 (1)	C17	0.0380 (3)	0.1865 (3)	0.2331 (5)	4.9 (1)
P1	0.20175 (7)	0.25560 (6)	0.4092 (1)	3.11 (2)	C18	0.1710 (3)	0.3430 (2)	0.3336 (4)	3.30 (9)
P2	0.63130 (8)	0.24497 (6)	0.0657 (1)	3.23 (2)	C19	0.2178 (3)	0.3593 (3)	0.2477 (4)	3.7 (1)
O1	0.4147 (2)	0.2596 (2)	0.6949 (3)	4.49 (7)	C20	0.1959 (3)	0.4256 (3)	0.1923 (4)	4.6 (1)
O2	0.0068 (2)	0.3117 (2)	0.5617 (3)	5.03 (8)	C21	0.1277 (4)	0.4776 (3)	0.2200 (4)	4.8 (1)
O3	0.1677 (2)	0.0274 (2)	0.7788 (3)	4.93 (8)	C22	0.0806 (4)	0.4627 (3)	0.3048 (5)	4.8 (1)
O4	0.2553 (3)	0.4304 (2)	0.6822 (4)	6.2 (1)	C23	0.1037 (3)	0.3964 (3)	0.3625 (4)	4.6 (1)
O5	0.4073 (2)	0.1268 (2)	0.9478 (3)	5.19 (8)	C24	0.4928 (3)	0.2683 (3)	0.2390 (4)	3.5 (1)
O6	0.3594 (3)	0.0223 (2)	0.5525 (3)	5.60 (9)	C25	0.7611 (3)	0.2343 (3)	0.3357 (4)	3.7 (1)
O7	−0.0264 (2)	0.1819 (2)	0.8162 (3)	6.33 (9)	C26	0.6524 (3)	0.4222 (3)	0.4952 (4)	3.8 (1)
O8	−0.0352 (3)	0.0723 (2)	0.4431 (3)	6.2 (1)	C27	0.6033 (3)	0.1387 (3)	0.2451 (4)	4.2 (1)
O9	0.2001 (3)	0.1776 (2)	1.0514 (3)	5.75 (9)	C28	0.5079 (3)	0.4380 (3)	0.2691 (4)	4.3 (1)
O10	0.3754 (2)	0.3537 (2)	0.9730 (4)	6.1 (1)	C29	0.4722 (3)	0.3635 (2)	0.4531 (4)	3.6 (1)
O11	0.0715 (2)	0.3816 (2)	0.8763 (4)	5.89 (9)	C30	0.8147 (3)	0.3961 (3)	0.3926 (4)	4.4 (1)
O24	0.4173 (2)	0.2439 (2)	0.1903 (3)	5.08 (8)	C31	0.7979 (3)	0.3223 (3)	0.5817 (4)	3.9 (1)
O25	0.8276 (2)	0.1969 (2)	0.3358 (3)	5.71 (9)	C32	0.5173 (3)	0.1883 (3)	0.4650 (4)	4.0 (1)
O26	0.6584 (2)	0.4752 (2)	0.5724 (3)	5.74 (9)	C33	0.6215 (3)	0.2973 (3)	0.6481 (4)	4.0 (1)
O27	0.5872 (3)	0.0721 (2)	0.2282 (4)	6.5 (1)	C34	0.7038 (3)	0.1725 (3)	0.5421 (4)	4.3 (1)
O28	0.4790 (3)	0.4875 (2)	0.2147 (4)	7.6 (1)	C35	0.6431 (3)	0.1535 (2)	−0.0343 (4)	3.18 (9)
O29	0.4168 (2)	0.3705 (2)	0.5072 (3)	5.20 (8)	C36	0.5929 (3)	0.1410 (3)	−0.1605 (4)	4.1 (1)
O30	0.8734 (2)	0.4312 (2)	0.3775 (3)	6.06 (9)	C37	0.5983 (4)	0.0690 (3)	−0.2351 (4)	5.2 (1)
O31	0.8463 (2)	0.3182 (2)	0.6796 (3)	5.36 (9)	C38	0.6530 (4)	0.0092 (3)	−0.1847 (5)	5.8 (1)
O32	0.4536 (2)	0.1488 (2)	0.4497 (3)	5.73 (9)	C39	0.7053 (4)	0.0209 (3)	−0.0607 (5)	5.3 (1)
O33	0.6223 (3)	0.3270 (2)	0.7464 (3)	6.1 (1)	C40	0.7000 (3)	0.0930 (3)	0.0147 (4)	4.1 (1)
O34	0.7570 (3)	0.1255 (2)	0.5777 (4)	6.9 (1)	C41	0.7195 (3)	0.3116 (3)	0.0504 (4)	3.9 (1)
C1	0.3386 (3)	0.2363 (2)	0.6767 (4)	3.32 (9)	C42	0.8042 (4)	0.2847 (3)	0.0301 (5)	5.7 (1)
C2	0.0718 (3)	0.2715 (2)	0.5901 (4)	3.46 (9)	C43	0.8720 (4)	0.3391 (4)	0.0269 (6)	7.4 (2)
C3	0.1748 (3)	0.0814 (3)	0.7335 (4)	3.5 (1)	C44	0.8546 (5)	0.4173 (3)	0.0428 (5)	7.1 (1)
C4	0.2337 (3)	0.3659 (3)	0.6564 (4)	3.7 (1)	C45	0.7701 (5)	0.4439 (3)	0.0594 (5)	7.3 (2)
C5	0.3547 (3)	0.1367 (3)	0.8561 (4)	3.51 (9)	C46	0.7031 (4)	0.3926 (3)	0.0638 (5)	5.9 (1)
C6	0.3249 (3)	0.0689 (2)	0.6101 (4)	3.8 (1)	H1T	0.191 (3)	0.184 (2)	0.582 (4)	5 (1)[b]
C7	0.0250 (3)	0.1802 (3)	0.7568 (4)	4.3 (1)	H1	0.285 (3)	0.234 (2)	0.384 (4)	5 (1)[b]
C8	0.0194 (3)	0.1082 (3)	0.5201 (4)	4.1 (1)	H2T	0.645 (3)	0.331 (2)	0.286 (4)	4.0 (9)[b]
C9	0.2025 (3)	0.2078 (3)	0.9691 (4)	3.8 (1)	H2	0.551 (2)	0.274 (2)	−0.004 (3)	3.1 (8)[b]

[a] Anisotropically refined atoms are given in the form of the isotropic equivalent thermal parameters: B (Å^2) $(4/3)[\beta_{11}a^2 + \beta_{22}b^2 + \beta_{33}c^2 + \beta_{12}ab \cos \gamma + \beta_{13}ac \cos \beta + \beta_{23}bc \cos \alpha]$. [b] Atoms were refined isotropically.

$C_{26}H_{30}Co_3O_{11}PRu$: C, 37.75; H, 3.65. Found: C, 37.5; H, 3.4.

Preparation of $HFeCo_3(CO)_{11}(PPh_3)$ (5a). To a solution of **1a** (0.200 g, 0.350 mmol) in CH_2Cl_2 (20 mL), was added PPh_3 (0.090 g, 0.343 mmol) in CH_2Cl_2 (10 mL), and the reaction mixture was stirred for 0.5 h at room temperature. The solution was filtered and the solvent was removed under reduced pressure. The resulting solid was first extracted with hexane to afford $HFeCo_3(CO)_{10}(PPh_3)_2$ as a green solid (0.020 g, 12%). Extraction with toluene gave black-violet microcrystals of **5a** (0.045 g, 35%). Anal. Calcd for $C_{29}H_{16}Co_3FeO_{11}P$: C, 43.32; H, 2.01. Found: C, 43.5; H, 2.2.

Preparation of $HFeCo_3(CO)_{11}(NMe_3)$ (6a). To a solution of **1a** (0.265 g, 0.465 mmol) in CH_2Cl_2 (20 mL), was added a solution of sublimed Me_3NO (0.035 g, 0.466 mmol) in CH_2Cl_2 (10 mL). Evolution of CO_2 occurred immediately and the violet reaction mixture became green. After 0.5 h of stirring at room temperature, the solution was filtered and the solvent was evaporated in vacuo. The resulting solid was washed with hexane (elimination of unreacted **1a**) and then extracted with toluene (80 mL). The toluene solution was evaporated to dryness, giving **6a** as a black powder (0.145 g, 52%). Anal. Calcd for $C_{14}H_{10}Co_3FeNO_{11}$: C, 27.99; H, 1.68; N, 2.33. Found: C, 28.4; H, 1.7; N, 2.5.

Preparation of $HFeCo_3(CO)_{11}(SEt_2)$ (7a). To a solution of **1a** (0.180 g, 0.315 mmol) in CH_2Cl_2 (20 mL), was added SEt_2 (0.034 mL, 0.314 mmol), and the reaction mixture was refluxed for 5 h. Chromatographic separation over silica gel using a hexane/toluene mixture (1:1) as eluent gave a purple band of unreacted **1a** followed by a deep violet band, which afforded **7a** as black crystals (0.060 g, 30%). Anal. Calcd for $C_{15}H_{11}Co_3FeO_{11}S$: C, 28.51; H, 1.75. Found: C, 28.9; H, 1.9.

Preparation of $HFeCo_3(CO)_{10}(NMe_3)(PPh_2H)$ (8a). To a solution of **2a** (0.180 g, 0.247 mmol) in CH_2Cl_2 (20 mL) was added a solution of sublimed Me_3NO (0.020 g, 0.266 mmol) in CH_2Cl_2 (20 mL). Evolution of CO_2 occurred immediately and the deep violet-red reaction mixture became green. After a few minutes of stirring at room temperature, the solution was filtered and the solvent was evaporated in vacuo. The resulting solid, first washed with hexane (elimination of residual **2a**), was extracted with toluene (40 mL). This solution was filtered and evaporated to dryness, giving **8a** as a green-black powder (0.085 g, 42%).

Preparation of $HFeCo_3(CO)_{10}(PPh_2H)(SEt_2)$ (9a). To a solution of **2a** (0.108 g, 0.148 mmol) in CH_2Cl_2 (20 mL), were added SEt_2 (0.016 mL, 0.149 mmol) and a solution of $Me_3NO{\cdot}2H_2O$ (0.016 g, 0.144 mmol) in CH_2Cl_2 (10 mL). The violet reaction mixture immediately became green. After a few minutes of stirring at room temperature, the solution was filtered and the solvent was evaporated in vacuo. The resulting solid was extracted with hexane (40 mL) and pure **9a** was obtained by cooling this solution to −15 °C. Black needles crystallized that were separated by filtration (0.055 g, 47%). Anal. Calcd for $C_{26}H_{22}Co_3FeO_{10}PS$: C, 39.52; H, 2.81. Found: C, 39.4; H, 2.6.

Preparation of $[HNEt_3][FeCo_3(CO)_{11}(PPh_2H)]$ (10a). To a solution of **2a** (0.050 g, 0.068 mmol) in CH_2Cl_2 (5 mL), was added NEt_3 (0.010 mL, 0.071 mmol). The violet solution, which rapidly became deep red, was stirred for few minutes at room temperature. After filtration, the solvent was evaporated in vacuo. The resulting solid was recrystallized from a hexane/CH_2Cl_2 mixture at −15 °C, affording the product as dark red needles (0.035 g, 62%).

Crystallographic Data, Structure Solution, and Refinement of 2a. Suitable black crystals of **2a** were obtained by slow crystallization of the compound from a hexane solution at −10

°C. Diffraction measurements were carried out at room temperature on a Nonius CAD-4 four-circle diffractometer, using graphite monochromatized Mo Kα radiation. Unit-cell parameters were calculated from the setting angles of 25 carefully centered reflections. Crystal data and intensity collections parameters are given in Table IV. The intensities of three reflections ($\bar{5}20$, $\bar{6}61$, $\bar{4}50$) were monitored every hour of exposure and showed no evidence of decay. For all subsequent computations the Enraf Nonius SPD package was used.[20] Data were corrected for Lorentz polarization but not for absorption. The crystal structure was solved by using the Patterson and Fourier difference methods and refined by full-matrix least squares with anisotropic thermal parameters for all non-hydrogen atoms. The function minimized was $\sum(w|F_o| - |F_c|)^2$, where the weight w is $[4F_o^2]/[\sigma^2(F_o) - (0.07|F_o|^2)]$. Hydrogen atoms were placed in calculated positions (C–H distances = 0.95 Å) in structure factor calculations and were assigned isotropic thermal parameters of $B = 5$ Å^2, except for H1, H1T, H2, and H2T, which were positioned by Fourier difference and refined isotropically. A final difference map revealed no significant residual peak. Neutral atom scattering factors used for all atoms and anomalous dispersion coefficients were obtained from standard sources.[21] The positional parameters obtained from the last cycle of refinement are listed in Table V, with the corresponding standard deviations.

Acknowledgment. We are grateful to Dr. F. Balegroune (Rennes) for her assistance with the X-ray study, to T. Richert (Strasbourg) for his contribution to the ^{59}Co NMR study, and to reviewers for drawing our attention to ref 2a,d,e. The Unité Mixte CNRS-Bruker-ULP thanks the "Region Alsace" for its participation in the purchase of the MSL 300 instrument and the Laboratoire de Chimie de Coordination is grateful to the "Commission of the European Communities" for financial support (Contract ST2J-0479-C).

Supplementary Material Available: Views of the structure of each molecule of **2a** in the asymmetric unit with the complete labeling scheme (Figure S-1) and a perspective view of the unit cell (Figure S-2), temperature factors for anisotropic atoms (Table S-I), a complete set of bond distances (Table S-II), and a complete set of bond angles (Table S-III) (12 pages); observed and calculated structure factor amplitudes for all observed reflections (Table S-IV) (29 pages). Ordering information is given on any current masthead page.

---

(20) Frenz, B. A. In *Computing in Crystallography*; Schenk, H., Olthof-Hazekamp, R., van Koningsveld, H., Bassi, G. C., Eds.; Delft University Press: Delft, The Netherlands, 1978; pp 64–71.

(21) *International Tables for X-Ray Crystallography*; Kynoch: Birmingham, 1974; Vol. IV, p 99.

Intramolecular Carbon–Carbon vs Carbon–Nitrogen Bond Formation in an Organopalladium Compound[†]

Nohma Beydoun and Michel Pfeffer*

Laboratoire de Chimie de Coordination, URA 416 du CNRS, Université Louis Pasteur,
4 Rue Blaise Pascal, F-67070 Strasbourg Cédex, France

André DeCian and Jean Fischer

Laboratoire de Cristallochimie et de Chimie Structurale, URA 424 du CNRS,
Université Louis Pasteur, 4 Rue Blaise Pascal, F-67070 Strasbourg Cédex, France

Received April 2, 1991

The reaction of the cyclopalladated compound of the 1,2,3,4-tetrahydro-1-(dimethylamino)naphthalene ligand, **2**, with 1 equiv of ethyl 3-phenylpropynoate leads to insertion of one alkyne into the Pd–C bond of **2**. The depalladation of this compound at reflux chlorobenzene temperature results in the synthesis of organic heterocyclic compounds. In the case of an iodated derivative the complete demethylation of the NMe$_2$ group is observed concomitantly with the C–N bond formation. The reaction of **2** with 2 equiv of diphenylacetylene leads to insertion of two alkynes into the Pd–C bond. The depalladation of this latter compound affords organic products containing a fulvene or a naphthyl ring via annulation of two phenyl units of the alkyne and an indolizinium derivative generated through intramolecular formation of a C–N bond by nucleophilic addition of an NMe$_2$ group to a polysubstituted alkene unit η^2-bonded to Pd.

Organopalladium compounds whose Pd–C bond is stabilized by intramolecular chelation of a nitrogen atom have led to interesting reactions with alkynes.[1] Thus, several syntheses of heterocyclic compounds have been observed, the C–N bond being formed by addition of the nitrogen atom to an activated alkene unit.[2] This latter possibility is however hampered by several side reactions that might take place at the alkyne substituents such as the annulation of aryl rings[3a–c] or the formation of pyrones by dealkylation of an ester function.[3d] It has for instance been established that depalladation of organopalladium compounds built up via reactions of the cyclopalladated (dimethylamino)methylphenyl ligand (referred to hereafter as "dmba") with two alkynes per Pd atom invariably led to the formation of organic compounds in which no C–N

[†] Reactivity of Cyclopalladated Compounds. 26. Part 25: Dupont, J.; Pfeffer, M.; Theurel, L.; Rotteveel, M. A.; De Cian, A.; Fischer, J. *New J. Chem.* **1991**, *15*, 551.

(1) Pfeffer, M. *Recl. Trav. Chim. Pays-Bas* **1990**, *109*, 567.

(2) (a) Maassarani, F.; Pfeffer, M.; Le Borgne, G. *Organometallics* **1987**, *6*, 2029. (b) Wu, G.; Rheingold, A. L.; Heck, R. F. *Organometallics* **1987**, *6*, 2386. (c) Wu, G.; Geib, S. J.; Rheingold, A. L.; Heck, R. F. *J. Org. Chem.* **1988**, *53*, 3238. (d) Pfeffer, M.; Rotteveel, M. A. *Recl. Trav. Chim. Pays-Bas* **1989**, *108*, 317.

(3) (a) Wu, G.; Rheingold, A. L.; Geib, S. J.; Heck, R. F. *Organometallics* **1987**, *6*, 1941. (b) Tao, W.; Silverberg, L. J.; Rheingold, A. L.; Heck, R. F. *Organometallics* **1989**, *8*, 2550. (c) Pfeffer, M.; Rotteveel, M. A.; Sutter, J. P.; De Cian, A.; Fischer, J. *J. Organomet. Chem.* **1989**, *371*, C21. (d) Pfeffer, M.; Rotteveel, M. A.; De Cian, A.; Fischer, J.; Le Borgne, G. *J. Organomet. Chem.* **1991**, *413*, C15.

0276-7333/91/2310-3693$02.50/0